encit 2020

ABCM
Associação Brasileira de Engenharia e Ciências Mecânicas

18th Brazilian Congress of Thermal Sciences and Engineering
November 16–20, 2020 (Online)

ENC-2020-0238
FLOW OF A CAPSULE SUSPENDED IN A NEWTONIAN LIQUID THROUGH A CONSTRICTED MICRO-CHANNEL

J. F. Roca
I. F. M. Menezes
M. S. Carvalho
Department of Mechanical Engineering, Pontifícia Universidade Católica do Rio de Janeiro, RJ 22453-900, Brazil
jroca@lmmp.mec.puc-rio.br
ivan@puc-rio.br
msc@lmmp.mec.puc-rio.br

Abstract. *Elastic capsules can be found in different applications, from red-blood cells in biological systems to flow in porous media. Study of the microscale phenomena is fundamental to assess the underlying macroscale dynamics. Thus, flow of a suspended capsule in a 2-D planar constricted micro-channel can be used as a model of the capsule flow through two adjacent pore-bodies connected by a pore-throat. The objective is to determine, for a given micro-channel, the maximum pressure peak as a function of different parameters, including elastic properties of capsule membrane and its pre-stress level, capsule radius, micro-channel geometry, liquid properties and flow conditions. The problem was solved using finite element and immersed boundary methods. Results showed that for a given micro-channel and flow conditions, a higher pressure peak is required to get the capsule deformed through the constriction as the capsule gets stiffer, and radius and pre-stress level increase.*

Keywords: *2-D micro-channel, fluid-structure interaction, immersed boundary method, finite element method.*

1. INTRODUCTION

A capsule is a closed fluid-filled membrane made by an elastic material (Rorai *et al.*, 2015). Capsules can be found in different natural and industrial applications, including transport of red-blood cell (RBC) on hemodynamics (Guido and Tomaiuolo, 2009), target delivery of drugs (Muzykantov, 2010), flow through porous media (do Nascimento *et al.*, 2017; Ribeiro, 2019), among others.

Flow through porous media is of special importance for this study. The injection of suspended capsules to reduce water phase mobility by blocking preferential paths and, in the process, diverting water to oil containing pores may lead to the increase of oil recovered (do Nascimento *et al.*, 2017; Ribeiro, 2019). In such problem, the study of the microscale phenomena is fundamental to understand the macroscopic dynamics. Thus, a constricted micro-channel is used as a model of a pore-throat connecting two adjacent pore-bodies. Flow of suspended capsules is a complex fluid-solid interaction problem, as comprehensive reviewed by Barthès-Biesel (2016).

Due to microscale, experimental analysis is extremely challenging. For that reason, numerical simulation can be utilized to address such problems by exploring a wide range of operating parameters, for instance. Among different numerical approaches, the immersed boundary method (IBM) was chosen in this study. Initially developed by Peskin (1972) to study flow patterns around heart valves, IBM uses an Eulerian-Lagrangian description at which the solid phase is considered as a part of the fluid domain, where an additional force is exerted. Mathematically, this force is described by the Dirac delta function δ_D, which defines a singular vector field that is different than zero only along the membrane.

Unlike other methods, finite element method does not require to approximate the Dirac delta function (Boffi and Gastaldi, 2003). Hence the effect of the solid on the fluid dynamics is computed through evaluating weighting functions at the Lagrangian points, whilst the membrane position is updated by using the fluid velocity field, configuring a *two-way interaction* problem.

Therefore, the main objective of this study is to simulate the flow of a suspended capsule in an incompressible Newtonian fluid through a constricted micro-channel, and determine how the pressure difference depends on different param-

eters, including capsule properties and dimensions, flow conditions, among others.

2. MATHEMATICAL DESCRIPTION

The constricted micro-channel Ω and the thin capsule membrane V are described using a 2-D Cartesian coordinates system. The flow domain is bounded by synthetic inlet and outlet planes, the symmetry plane and the channel wall, described by a cosine function.

$$H(x) = \frac{H_s}{2}\left[(1+\beta) + (1-\beta)cos\left(2\pi\frac{x}{L}\right)\right], \tag{1}$$

where L is the channel length, H_s and H_0 are the maximum and minimum channel height, as indicated in Fig. 1. $\beta \equiv H_0/H_s$ is the constriction ratio.

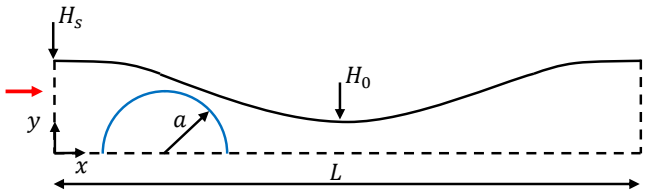

Figure 1. Sketch of the flow domain.

For an incompressible viscous fluid, momentum and mass conservation equations in an Eulerian frame are written as

$$\begin{aligned} \rho\left(\frac{\partial \mathbf{u}}{\partial t} + \mathbf{u}.\boldsymbol{\nabla}\mathbf{u}\right) &= \boldsymbol{\nabla}.\boldsymbol{\tau} + \mathbf{f}^{\mathbf{B}}, \\ \boldsymbol{\nabla}.\mathbf{u} &= 0, \end{aligned} \tag{2}$$

where t, ρ, $\mathbf{u} = (u, v)$, $\boldsymbol{\tau}$ and $\mathbf{f}^{\mathbf{B}}$ are time, density, velocity vector, stress tensor, and body force associated with the fluid-solid interaction, respectively. For incompressible Newtonian fluids, the stress tensor is defined as

$$\boldsymbol{\tau} = -p\mathbf{I} + \mu[\boldsymbol{\nabla}\mathbf{u} + (\boldsymbol{\nabla}\mathbf{u})^T], \tag{3}$$

where p and μ are pressure and dynamic viscosity, respectively.

It is worth noting that the capsule thickness is small compared to other dimensions. No twisting and bending moments are considered, as well as no shear stress. Thus, only stretching and compression of the capsule membrane are computed. The interaction between the capsule membrane and the fluid can be modeled through the body force $\mathbf{f}^{\mathbf{B}}$ in the momentum equation, which represents the force that the membrane exerts on the fluid. It is described as a volume integral along the solid volume V as follows (Peskin, 1972),

$$\mathbf{f}^{\mathbf{B}}(\mathbf{x}) = \int_V \mathbf{f}\delta_D(\mathbf{x} - \mathbf{X})\, dV', \tag{4}$$

where $\mathbf{x}$ is an independent variable in the Eulerian frame, $\mathbf{X}$ is the position of solid domain and δ_D is the Dirac delta function. Hence the body force $\mathbf{f}^{\mathbf{B}}$ is a singular vector field, zero everywhere except on the membrane.

In the 2-D planar flow, coordinates of the membrane points $\mathbf{X}$ can be written as $\mathbf{X} = \mathbf{X}(s, t)$, where s is the arc-length, as illustrated in Fig. 2.

In order to obtain $\mathbf{f}$, a free-body diagram of the membrane element is drawn in Fig. 2, including forces along s-direction and the force exerted on the membrane element $\mathbf{F}_{\mathbf{fluid/solid}}$. Thus, forces along s-direction acting on the surface area $h \times 1$, where h is the membrane thickness, can be balanced as

$$\left(T + \frac{\partial T}{\partial s}\delta s\right)\left(\mathbf{t} + \frac{\partial \mathbf{t}}{\partial s}\delta s\right)h - T\mathbf{t}h. \tag{5}$$

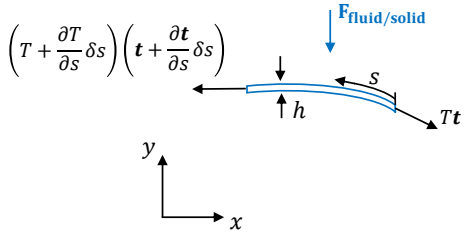

Figure 2. Free-body diagram of the 1-D membrane element includes forces exerted on the element by the surrounding fluid and forces along s-direction (gravity force neglected).

Considering a massless membrane element and that the second order terms $(\delta s)^2$ are neglected, the net force along s-direction balances the force exerted on the solid $\mathbf{F_{fluid/solid}}$ as follows

$$\frac{\partial(T\mathbf{t})}{\partial s}\delta s h + \mathbf{F_{fluid/solid}} = \mathbf{0}, \tag{6}$$

recalling that $\mathbf{F_{fluid/solid}} = -\mathbf{F_{solid/fluid}}$ and dividing Eq. (6) by $\delta V = \delta s_1 \times 1 \times h$, the force per unit volume $\mathbf{f}$ is finally obtained:

$$\mathbf{f} = \frac{\partial(T\mathbf{t})}{\partial s}, \tag{7}$$

where unit tangent vector $\mathbf{t}$ is defined along the membrane direction s (Peskin and McQueen, 1989).

Considering that the membrane material follows Hooke's law, T depends linearly on the strain ε:

$$T(\mathbf{X}(\mathbf{s},\mathbf{t})) = \left(\frac{E}{1-\nu^2}\right)\varepsilon, \tag{8}$$

where E and ν are the Young's modulus and Poisson's ratio of the membrane material, respectively. The strain ε is defined as the ratio of the deformation over the unstressed arc-length s_0 of a membrane element, and calculated for an unstressed reference configuration as $\varepsilon = \left|\frac{\partial \mathbf{X}}{\partial s_0}\right| - 1$ (Peskin and McQueen, 1989).

Considering initial state at $t = 0$ and pre-stressed tension T_0 (Evans and Skalak, 2018), T can be explicitly expressed for any time t as

$$T(\mathbf{X}(s,t)) = \left(\frac{E}{1-\nu^2}\right)\left(\frac{s(t) - s(t=0)}{s_0}\right) + T_0, \tag{9}$$

where $s(t)$, $s(t=0)$ and s_0 are arc-length of the membrane element at any time t, time $t = 0$, and at the unstressed state, respectively.

The pre-stressed tension T_0, which defines the initial pressure difference between inner and outer phases, is expressed as

$$T_0 = \alpha\left(\frac{E}{1-\nu^2}\right), \tag{10}$$

where α is the pre-inflation parameter, defined as $\alpha = \frac{a}{a_0} - 1$ (Lefebvre and Barthès-Biesel, 2007).

The capsule membrane position $\mathbf{X}$ is then advected by the velocity field considering no-slip condition:

$$\begin{aligned}\frac{\partial \mathbf{X}}{\partial t} &= \int_\Omega \mathbf{u}\delta_D(\mathbf{x}-\mathbf{X})\, d\Omega' \\ &= \mathbf{u}(\mathbf{X},t).\end{aligned} \tag{11}$$

2.1 Boundary and initial conditions

At the inlet plane, a parabolic velocity profile is imposed:

$$u(x=0,y)=\frac{3\overline{V}}{2}\left[1-\left(\frac{y}{H_s}\right)^2\right],\ v(x=0,y)=0, \tag{12}$$

where $\overline{V}$ is the average velocity of the continuous phase and H_s is the half the channel height at the inlet, as shown in Fig. 1.

At the outflow plane, a fully developed flow and a fixed outflow pressure are imposed:

$$\mathbf{n}.\boldsymbol{\nabla}\mathbf{u}\big|_{x=L}=\mathbf{0},\ p_{out}=0. \tag{13}$$

At the wall, no-slip/no-penetration condition is imposed: $\mathbf{u}=\mathbf{0}$. Along the symmetry plane, zero vertical velocity and zero tangential stress are considered:

$$v=0,\ \mathbf{t}.(\boldsymbol{\tau}.\mathbf{n})=0, \tag{14}$$

where $\mathbf{t}$ and $\mathbf{n}$ are unit tangent vector and unit normal vector at the symmetry plane, respectively.

In order to ensure symmetry of the capsule, a geometric constraint is imposed on the extreme points of the solid domain, at $s=0$ and $s=l_s(t)$.

$$\left.\frac{\partial X}{\partial s}\right|_{s=0,l_s(t)}=0, \tag{15}$$

where $\mathbf{X}=(X,Y)$ defines the capsule membrane geometry and $l_s(t)$ is the solid domain length at any time t. Finally, at $t=0$, zero velocity and pressure fields are defined, whereas the capsule center is known and pre-stressed condition is defined by the pre-inflation parameter α.

3. NUMERICAL SOLUTION

Regarding the numerical solution, the finite element method coupled with the immersed boundary method have been used to solve momentum and continuity conservation equations. Time integration scheme utilized a predictor-corrector algorithm. Nonlinearities are addressed using Newton's method (further details in Carvalho and Valério (2012)). The system of algebraic equations is LU factorized using the MATLAB® solver.

The coupling between both fluid and solid domains is addressed by using two different grids. A fixed grid made by quadrilateral elements to define the fluid domain, whilst a movable and flexible grid conformed by linear segments to define the solid domain. The effect of the membrane on the fluid domain is taken into account by including an additional term at the momentum conservation equation, and its respective weighted residual as follows

$$R_{mi}^{\mathbf{fB}}=-\int_{\Omega}\mathbf{f}^{\mathbf{B}}.\mathbf{W_i}\,d\Omega', \tag{16}$$

where $R_{mi}^{\mathbf{fB}}$ is the additional term in the momentum residual to couple fluid flow and membrane dynamics, and $\mathbf{W_i}$ is the weighting function.

Substituting Eq. (4) into Eq. (16) yields

$$R_{mi}^{\mathbf{fB}}=-\int_{\Omega}\int_{V}\mathbf{f}\delta_D(\mathbf{x}-\mathbf{X})dV'.\mathbf{W_i}\,d\Omega'=-\int_{V}\mathbf{f}.\mathbf{W_i}(\mathbf{X})\,dV'. \tag{17}$$

Combining Eqs. (7) and (17), and after integrating by parts, the following expression is obtained

$$R_{mi}^{\mathbf{fB}} = -T_1 \mathbf{t_1}.\mathbf{W_i}(\mathbf{X})h\Big|_0^{l_s(t)} + \int_0^{l_s(t)} T_1 \mathbf{t_1}.h\, d\mathbf{W_i}(\mathbf{X}), \tag{18}$$

which reduces the fluid-solid interaction force to a line integral along the capsule membrane.

Finally, time evolution of membrane position is computed by advection using the velocity field.

4. RESULTS AND DISCUSSION

The objective is to determine the pressure time evolution $\Delta P(t) = p_{in}(t) - p_{out}$ for different flow conditions and capsule properties. This problem is governed by different parameters including: the dimensionless capsule radius $\overline{a} = a/H_0$, the constriction ratio $\beta = H_0/H_s$, the surface capillary number $Ca_s = \mu\overline{V}/G_s$ and the Reynolds number $Re = \rho\overline{V}2H_s/\mu$. In addition, G_s known as the surface shear modulus, is defined as $\frac{Eh}{2(1+\nu)}$ (Carroll, 2014; Dupont *et al.*, 2015).

A single micro-channel was studied. Entrance and constriction channel heights are $H_s = 0.5\ mm$ and $H_0 = 0.215\ mm$. Channel length $L = 4.5\ mm$. The mesh has 27×243 quadrilateral elements and 238 Lagrangian points to define the 1-D membrane.

The inner and outer liquid phases are the same, with $\rho = 1000\ kg/m^3$ and $\mu = 0.001\ Pa.s$. The membrane material has $\nu = 0.499$ and $h = 0.01\ mm$. Three different pre-inflation parameters, $\alpha = 0.025,\ 0.05,\ 0.1$ are explored.

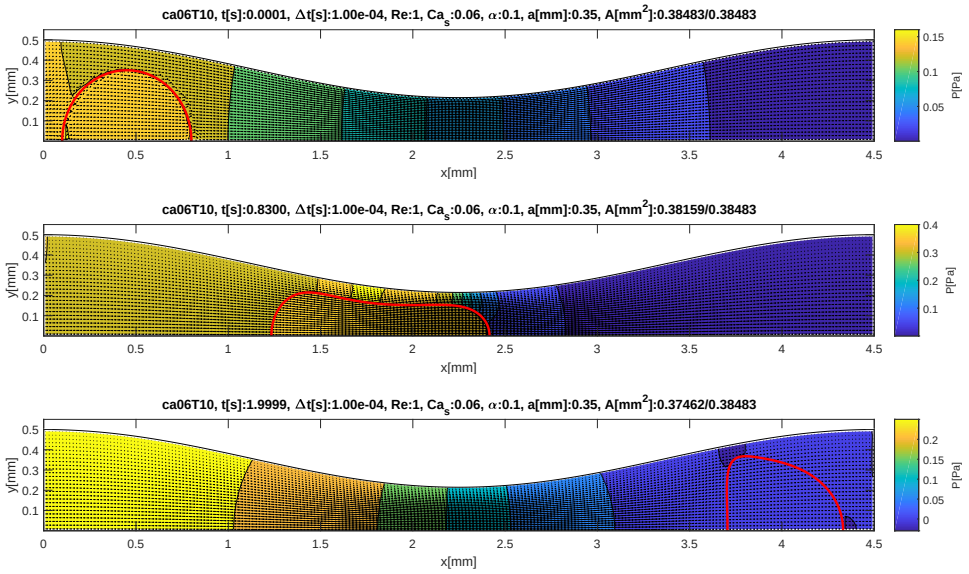

Figure 3. Time evolution of the membrane, velocity and pressure fields: a) $t = 0.001\ s$, b) $t = 0.83\ s$, and c) $t = 1.999\ s$. $Re = 1.0$, $Ca_s = 0.06$, $\alpha = 0.1$ and $\overline{a} = 1.63$.

Figure 3 shows the temporal evolution of the flow field and capsule configuration as it flows through the 2-D constricted micro-channel, at $Re = 1.0$, $Ca_s = 0.06$, $\alpha = 0.1$ and $\overline{a} = 1.63$. As flow starts, the capsule moves towards the throat and deforms. The inlet pressure starts to rise in order to get the membrane deformed through the constriction, reaching its maximum when the capsule tip reaches the minimum channel height. The inlet pressure falls as the capsule flows through the diverging section of the channel.

Figure 4 illustrates the pressure evolution for different Ca_s. The inlet pressure for a single-phase flow is the black continuous line, which is the solution for $Ca_s \to \infty$. As expected, the lower the Ca_s, the higher the pressure peak, showing the key role played by the stiffness of capsule material.

We can change two other parameters such as the pre-inflation parameter α and dimensionless capsule radius $\overline{a}$, in order to obtain the dependence of maximum pressure peak. This is obtained by the blocking factor f (Cobos *et al.*, 2009), defined as the ratio of the pressure difference of the single-phase flow to the maximum pressure difference of the capsule flow at the same Reynolds number Re. This blocking factor can characterize the flow mobility reduction. A lower value of f corresponds to a flow condition at which the elastic capsule strongly blocks the pore, whereas a higher value of f means that the capsule has a weak effect on blocking. Figure 5 depicts the mobility factor f as a function of surface capillary number Ca_s and pre-inflation parameter α. The effectiveness of blocking mechanism depends on low enough Ca_s. Thus, for a given $\overline{a}$ and a pre-inflation parameter α, the lower Ca_s, the lower the factor f. Similarly, for a given value of Ca_s and pre-inflation parameter α, the larger the capsule, the lower the factor f.

5. FINAL REMARKS

The flow of a suspended capsule, modeled as a 1-D membrane, through a 2-D planar constricted micro-channel was presented. This study used finite element method with immersed boundary method. The effect of the membrane on fluid dynamics was computed through an additional term in the Navier-Stokes equations. Results showed the influence of the pre-inflation parameter α, the surface capillary number Ca_s, the dimensionless capsule radius $\overline{a}$ on the blocking factor f for a given Reynolds number Re.

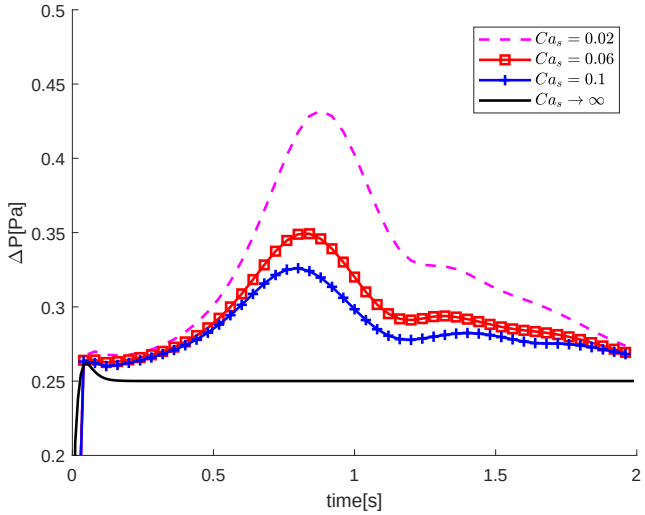

Figure 4. Evolution of the injection pressure for different Ca_s at $Re = 1.0$, $\alpha = 0.1$ and $\overline{a} = 1.63$.

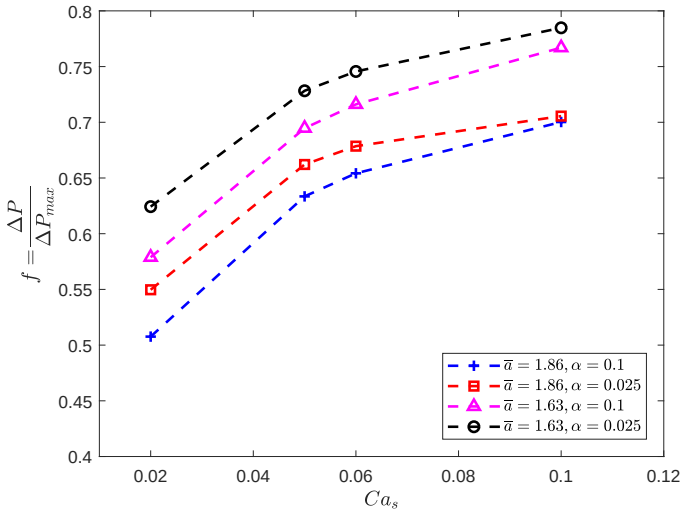

Figure 5. Blocking factor as a function of Ca_s for different dimensionless capsule radii $\overline{a}$ and pre-inflation parameters α at $Re = 1.0$.

6. ACKNOWLEDGEMENTS

This study was financed in part by the Coordenação de Aperfeiçoamento de Pessoal de Nível Superior - Brasil (CAPES) - Finance Code 001. Furthermore, it was carried out in association with the project registered as Escoamento de dispersões complexas em meios porosos heterogêneos: análise na escala de poro e macroscópica (PUC-Rio/BG Brasil/Shell Brasil/ANP) - Complex Dispersion Flow Through Porous Media - funded by BG Brasil/Shell Brasil under the ANP R&D levy as *Compromisso de Investimentos com Pesquisa e Desenvolvimento*.

7. REFERENCES

Barthès-Biesel, D., 2016. "Motion and deformation of elastic capsules and vesicles in flow". *Annu. Rev. Fluid Mech.*, Vol. 4, pp. 25–52.

Boffi, D. and Gastaldi, L., 2003. "The immersed boundary method: a finite element approach". *Computational Fluid and Solid Mechanics*, Vol. 7, pp. 1263–1266.

Carroll, R., 2014. *Computational study of droplet and capsule flow in channels with inertial effect*. Ph.D. thesis, University of New Hampshire.

Carvalho, M. and Valério, J., 2012. *Introdução ao método de elementos finitos: Aplicação em dinâmica dos fluidos*, Vol. 61. SBMAC, São Carlos, São Paulo. ISBN 978-85-8215-012-2.

Cobos, S., Carvalho, M. and Alvarado, V., 2009. "Flow of oil–water emulsions through a constricted capillary". *Internal Journal of Multiphase Flow*, Vol. 35, No. 6, pp. 507–515.

do Nascimento, D., Avendano, J., Mehl, A., Moura, M., Carvalho, M. and Duncanson, W., 2017. "Flow of tunable elastic microcapsules through constrictions". *Scientific Reports*.

Dupont, C., Tallec, P., Barthès-Biesel, D., Vidrascu, M. and Salsac, A.V., 2015. "Dynamics of a spherical capsule in a planar hyperbolic flow: influence of bending resistance". *Procedia IUTAm*, Vol. 16, pp. 70–79.

Evans, E. and Skalak, R., 2018. *Mechanics and thermodynamics of biomembranes*. CRC Press Taylor & Francis Group, Boca Raton, Florida.

Guido, S. and Tomaiuolo, G., 2009. "Microconfined flow behavior of red blood cells in vitro". *Comptes Rendus Physique*, Vol. 10, No. 8, pp. 751–763.

Lefebvre, Y. and Barthès-Biesel, D., 2007. "Motion of a capsule in a cylindrical tube: effect of membrane pre-stress". *J. Fluid Mech*, Vol. 589, pp. 157–181.

Muzykantov, V., 2010. "Drug delivery by red blood cells: vascular carriers designed by mother nature". *Comptes Rendus Physique*, Vol. 7, No. 4, pp. 403–427.

Peskin, C., 1972. "Flow patterns around heart valves: A numerical method". *Journal of Computational Physics*, Vol. 10, pp. 252–271.

Peskin, C. and McQueen, D., 1989. "A three-dimensional computational method for blood blow in heart i. immersed elastic fibers in a viscous incompressible fluid". *Journal of Computational Physics*, Vol. 81, pp. 372–405.

Ribeiro, R.C.S., 2019. *3-D Visualization of Oil Displacement by a Suspension of Microcapsules*. Master's thesis, Pontifícia Universidade Católica do Rio de Janeiro.

Rorai, C., Touchard, A., Zhu, L. and Brandt, L., 2015. "Motion of an elastic capsule in a constricted microchannel". *The European Physical Journal E*, Vol. 38, No. 5, p. 49.

8. RESPONSIBILITY NOTICE

The authors are solely responsible for the printed material included in this paper.